Environmental Science & Technology

Article

pubs.acs.org/est

High Contribution of Nonfossil Sources to Submicrometer Organic Aerosols in Beijing, China

Yanlin Zhang,[*,†] Hong Ren,[‡,○] Yele Sun,[‡,○] Fang Cao,[†] Yunhua Chang,[†] Shoudong Liu,[†] Xuhui Lee,[†,◆] Konstantinos Agrios,[§,∥] Kimitaka Kawamura,[⊥] Di Liu,[#] Lujie Ren,[▽] Wei Du,[‡,○] Zifa Wang,[‡] André S. H. Prévôt,[∥] Sönke Szidat,[§] and Pingqing Fu[*,‡,▽,○]

[†]Yale-NUIST Center on Atmospheric Environment, International Joint Laboratory on Climate and Environment Change (ILCEC), Nanjing University of Information Science and Technology, Nanjing 210044, China

[‡]LAPC, Institute of Atmospheric Physics, Chinese Academy of Sciences, Beijing 100029, China

[§]Department of Chemistry and Biochemistry & Oeschger Centre for Climate Change Research, University of Bern, Bern 3012, Switzerland

[∥]Paul Scherrer Institute (PSI), Villigen-PSI 5232, Switzerland

[⊥]Institute of Low Temperature Science, Hokkaido University, Sapporo 060-0819, Japan

[#]School of Geography, Earth and Environmental Sciences, University of Birmingham, Birmingham, B15 2TT, United Kingdom

[▽]Institute of Surface-Earth System Science, Tianjin University, Tianjin 300072, China

[○]College of Earth Sciences, University of Chinese Academy of Sciences, Beijing 100049, China

[◆]School of Forestry and Environmental Studies, Yale University, New Haven, Connecticut United States

ABSTRACT: Source apportionment of organic carbon (OC) and elemental carbon (EC) from PM_1 (particulate matter with a diameter equal to or smaller than 1 μm) in Beijing, China was carried out using radiocarbon (^{14}C) measurement. Despite a dominant fossil-fuel contribution to EC due to large emissions from traffic and coal combustion, nonfossil sources are dominant contributors of OC in Beijing throughout the year except during the winter. Primary emission was the most important contributor to fossil-fuel derived OC for all seasons. A clear seasonal trend was found for biomass-burning contribution to OC with the highest in autumn and spring, followed by winter and summer. ^{14}C results were also integrated with those from positive matrix factorization (PMF) of organic aerosols from aerosol mass spectrometer (AMS) measurements during winter and spring. The results suggest that the fossil-derived primary OC was dominated by coal combustion emissions whereas secondary OC was mostly from fossil-fuel emissions. Taken together with previous ^{14}C studies in Asia, Europe and USA, a ubiquity and dominance of nonfossil contribution to OC aerosols is identified not only in rural/background/remote regions but also in urban regions, which may be explained by cooking contributions, regional transportation or local emissions of seasonal-dependent biomass burning emission. In addition, biogenic and biomass burning derived SOA may be further enhanced by unresolved atmospheric processes.

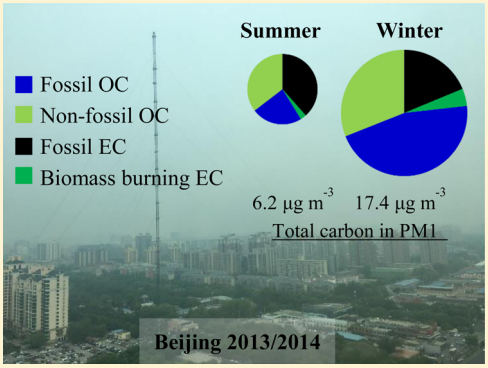

1. INTRODUCTION

Carbonaceous aerosols, which can contribute 20−90% of the total fine aerosol mass concentrations[1,2] are of great importance due to their significant and complex impacts on air quality, human health and climate.[3−5] According to different physical and chemical properties, bulk carbonaceous aerosols (total carbon, TC) are operationally divided into two subfractions namely organic carbon (OC) and elemental carbon (EC) or black carbon (BC) when carbonate carbon (CC) may be negligible or less than 5% of the TC mass in fine (i.e., $PM_{2.5}$, particulate matter with a diameter equal to or smaller than 2.5 μm) or submicrometer particulate matter (PM_1).[6] PM_1 may be more important to human health compared to $PM_{2.5}$ because smaller particles may have higher ability to penetrate into the human respiratory system.[7] OC can scatter or reflect solar light leading to a net cooling effect on the Earth' climate, whereas EC can significantly contribute to global warming due to its light absorbing behavior.[5] OC and EC not only differ in their chemical and environmental effects but also differ in their origins and formation.[6,8] OC can be emitted as primary OC (POC) and formed as secondary OC (SOC) through gas-to-particle conversion after gas-phase oxidation of volatile organic precursors or aqueous-phase processing of low-molecular-

Received: March 24, 2017
Revised: June 20, 2017
Accepted: June 23, 2017
Published: June 24, 2017

DOI: 10.1021/acs.est.7b01517
Environ. Sci. Technol. 2017, 51, 7842−7852

weight water-soluble organic compounds.[6,8−10] EC almost exclusively originates from incomplete combustion either from fossil-fuel combustion or biomass burning.[11] POC and its precursors can be emitted from fossil (e.g., coal combustion and vehicle exhaust) and nonfossil sources (e.g., biomass burning, vegetation emissions, cooking).[8,12−14] Several studies have revealed that OC and EC differ in their origins and formation processes based on bottom-up and top-down approaches,[15−18] and it is therefore very challenging to quantitatively determine contributions from different sources to OC and EC separately, especially in polluted urban regions.

Beijing, the capital of China, is one of largest megacities in the world with a population of 20 million over an area of 16 800 km^2 and it has faced serious air pollution problems for the last decades. Zheng et al. (2015) found that $PM_{2.5}$ is associated with an average total mortality of 5100 individuals per year for the period 2001−2012 in Beijing, and their results underscored the urgent need for air pollution abatement in Beijing or similar polluted megacities and city clusters.[19] Extensive studies have been conducted in recent years to characterize severe haze pollution.[20−22] However, most of them were focused on pollution episodes, an individual season or specific seasons for comparisons (e.g., summer vs winter; heating vs nonheating season).

Recent studies have shown that radiocarbon (^{14}C) measurements can unambiguously determine fossil and nonfossil sources of carbonaceous particles, because ^{14}C is completely depleted in fossil-fuel emissions due to its age (half-life 5730 years), whereas nonfossil carbon sources (e.g., biomass burning, cooking, or biogenic emissions) show a contemporary ^{14}C content.[23,24] Moreover, a better ^{14}C-based source apportionment can be obtained when ^{14}C determinations are performed on OC, EC, and water-soluble OC.[23,25−28] Biomass burning, coal combustion, vehicle emission, cooking, and the secondary formation from anthropogenic and biogenic precursors have been identified as important sources of fine particle in Beijing.[21,29−35] Recent applications of the positive matrix factorization (PMF) algorithm with aerosol mass spectrometer measurement (AMS-PMF) from field campaigns have revealed a predominance of oxygenated organic aerosol (OOA) over hydrocarbon-like OA (HOA) in various atmospheric environments, although their fossil/nonfossil sources still remain relatively unknown.[2,34−37]

It should be noted that most of these aerosol mass spectrometer studies have been conducted for PM_1. A full yearly variation of relative fossil and nonfossil contribution of different carbonaceous aerosols in PM_1 in Beijing is urgently needed. To the best of our knowledge, this study is the first time that ^{14}C-based source apportionment of PM_1 is simultaneously carried out in different carbonaceous fractions during four seasons in Beijing to attain a comprehensive picture of the source and formation information on carbonaceous aerosols. In addition, ^{14}C results were also combined with AMS-PMF results to quantify the fossil and nonfossil contributions to oxygenated organic carbon (OOC, a surrogate for SOC) and assess contributions to POC from different sources (cooking, biomass burning, coal combustion, hydrocarbon-like OC). Finally, the data set is also complemented by previous ^{14}C-based source apportionment studies conducted in urban, rural and remote regions in the Northern Hemisphere to gain an overall picture of the sources of OC aerosols.

2. EXPERIMENTAL SECTION

2.1. Sampling. PM_1 samples were collected on the rooftop of a two-floor building (8 m a.g.l.) located at the State Key Laboratory of Atmospheric Boundary Layer Physics and Atmospheric Chemistry (LAPC), Institute of Atmospheric Physics (IAP), Chinese Academy of Sciences in Beijing, China. The samples were collected onto prebaked quartz fiber filters (Pallflex) by a gravimetric volume sampler (Zambelli, Italy) at a flow rate of 38.7 L min^{-1} for around 3 days for each sample from 28 July 2013 to 21 April 2014. For each season, 10−15 samples were collected. Blank was collected during each season with the pump off during the sampling. The filters were previously enveloped with aluminum foils and then baked at 450 °C for 6 h before sampling. After sampling, each filter was packed separately stored in a refrigerator under −20 °C until the analysis.

2.2. Thermal-Optical Carbon Analysis. OC and EC mass concentrations were measured by the NIOSH thermal-optical transmission (TOT) protocol.[38] The replicate analysis of samples (every 10 samples) showed a good analytical precision with relative standard deviations of 5.2%, 9.5%, and 5.2% for OC, EC and TC, respectively. The average field blank of OC was 1.9 ± 1.0 $\mu g/cm^2$ (n = 4, equivalent to ∼0.3 ± 0.15 $\mu g/m^3$), which was subtracted from the measured OC concentrations. A corresponding EC blank was not detectable.

2.3. ^{14}C Analysis of the Carbonaceous Fractions. One to three sequent filter samples were pooled together for ^{14}C measurement. The method of ^{14}C measurement of carbonaceous aerosols was described elsewhere.[13,39,40] In short, ^{14}C of TC was analyzed by coupling of an elemental analyzer (EA) with a MIni CArbon Dating System (MICADAS) at the University of Bern, Switzerland.[41,42] ^{14}C analysis of EC was carried out by online coupling the MICADAS with a Sunset Lab OC/EC analyzer[43] where CO_2 evolved from the EC peak is separated after OC was combusted from the filter sample (1.5 cm^2) by TOT Swiss_4S protocol.[39] Two samples with relatively high concentrations for each season were selected for ^{14}C measurements of water-soluble OC (WSOC). The mass and f_M values of WSOC were deduced from subtraction of OC and water-insoluble OC (WIOC) based on mass and isotope-mass balancing. ^{14}C measurement of WIOC was measured under the same conditions as OC after water extraction of the filter.[26]

^{14}C results were expressed as fractions of modern (f_M), that is, the fraction of the $^{14}C/^{12}C$ ratio of the sample related to that of the reference year 1950.[44] f_M(EC) for each sample was further corrected by EC loss (20 ± 8% on average) during the OC removal steps and possibly positive EC artifact from OC charring (10 ± 6% of EC on average) similar to previous analyses.[39,45] f_M(TC) was corrected for field blanks. The mean uncertainties of f_M(EC) and f_M(TC) were 5% and 2%, respectively. ^{14}C results in OC (f_M(OC)) were then calculated indirectly according to an isotope mass balance:[40]

$$f_M(\mathrm{OC}) = \frac{\mathrm{TC} \times f_M(\mathrm{TC}) - \mathrm{EC} \times f_M(\mathrm{EC})}{\mathrm{TC} - \mathrm{EC}}$$

The uncertainty of f_M(OC) estimated by this approach is on average 8% obtained from an error propagation and includes all the individual uncertainties of f_M(TC) (2%), f_M(EC) (5%), TC (8%), and EC (25%).

Nonfossil fractions of OC and EC (i.e., f_{NF}(OC) and f_{NF}(EC), respectively) were determined from the f_M values and

DOI: 10.1021/acs.est.7b01517
Environ. Sci. Technol. 2017, 51, 7842−7852

reference values for pure nonfossil sources: $f_{NF} = f_M(\text{sample})/f_M(\text{REF})$. The estimation of reference values ($f_M(\text{REF})$) have been previously reported in details.[26,39,46] $f_M(\text{REF})$ values amount to 1.07 ± 0.04 and 1.10 ± 0.05 for OC and EC, respectively by a tree-growth model with a long-term $^{14}CO_2$ measurement[47] and by assuming that biomass burning contribution to nonfossil OC and EC is 50 ± 25% and 100%, respectively. It should be noted that the uncertainties of references values of $f_{NF}(\text{ref})$ were relatively small compared to uncertainties from overall source-apportionment calculation. Uncertainties were determined by error propagation of all individual uncertainties including OC and EC mass concentrations, ^{14}C results of OC and EC, $f_M(\text{REF})$ as well as corrections for field blanks, EC recovery and charring. The overall average uncertainties of f_{NF} were estimated as 5% (i.e., ranging from 3% to 7%) for OC and 8% (4% to 12%) for EC. Indeed, blank corrections and EC yield corrections are the most important contributors to the total uncertainties of OC and EC, respectively.

2.4. HR-ToF-AMS Operation and PMF. An Aerodyne High-resolution Time-of-Flight Aerosol Mass Spectrometer (HR-ToF-AMS) was deployed at the same location for real-time measurements of nonrefractory submicron species, including organic aerosols, sulfate, nitrate, ammonium, and chloride in spring (8−28 March, 2014) and winter (17 December 2013 to 17 January, 2014). The detailed setup and operations of the HR-ToF-AMS is given elsewhere.[22] The high-resolution mass spectra were then analyzed to determine the elemental ratios of OA, for example, organic-mass to organic-carbon (OM/OC) and oxygen-to-carbon (O/C), using the Improved-Ambient method,[48] and OC mass was calculated as [OA]/[OM/OC]. Positive matrix factorization (PMF) was performed to high-resolution OA spectra to resolve potential source factors in spring and winter. After careful evaluations of the mass spectral profiles and times series following the procedures described elsewhere,[49] six factor solution was chosen for both spring and winter studies, which included a hydrocarbon-like OA (HOA), cooking OA (COA), biomass burning OA (BBOA), coal combustion OA (CCOA), and two oxygenated OA factors, that is, less oxidized OOA (LO-OOA) and more oxidized OOA (MO-OOA). The OC mass for each factor such as hydrocarbon-like OC (HOC), cooking OC (COC), biomass burning OC (BBOC), coal combustion OC (CCOC), and oxidized OOA (OOC) was calculated by dividing the corresponding OM/OC ratio. A more detailed PMF analysis and data interpretation has been given.[22]

2.5. ^{14}C-Based Source Apportionment Model. An advanced ^{14}C-based source apportionment model was used to quantify OC and EC from each source, which was achieved by the Latin-Hypercube Sampling (LHS) simulations using the data set from mass concentrations of OC and EC, estimated primary emission ratios for fossil fuel and biomass burning as well as ^{14}C results (termed as the ^{14}C-LHS method).[40] In total, four major sources were resolved including EC from fossil and nonfossil sources (EC_{FF} and EC_{NF}, receptively), OC from fossil and nonfossil sources (OC_{FF} and OC_{NF}, receptively). OC_{FF} and OC_{NF} were further apportioned into subfractions of fossil-fuel OC from primary (POC_{FF}) and secondary organic carbon (SOC_{FF}) and nonfossil OC from primary biomass-burning sources (POC_{BB}) and other nonfossil (ONF) sources (e.g., cooking and primary/secondary nonfossil OC, OC_{ONF}). The equations for the detailed source apportionment are shown in Table 1. Central (median) values with low and high limits were used as input parameters, and all solutions were included in frequency distributions of possible solutions except those producing negative values.

Table 1. Equations for ^{14}C-Based Source Apportionment Model, See Sec 2.5 for the Details

equations
$EC_{NF} = f_{NF}(EC) \times EC$
$EC_{FF} = EC - EC_{NF}$
$OC_{NF} = f_{NF}(OC) \times OC$
$OC_{FF} = OC - OC_{NF}$
$POC_{FF} = EC_{FF}/(EC/POC)_{FF}$
$SOC_{FF} = OC_{FF} - POC_{FF}$
$POC_{BB} = EC_{NF}/(EC/POC)_{BB}$
$OC_{ONF} = OC_{NF} - POC_{BB}$
$OC_{AMS} = OA_{AMS}/(OM/OC)_{AMS}$

The median values of $(EC/POC)_{BB}$ amounted to 0.3 with a range from 0.1 (low limit) to 0.5 (high limit), according to composed emission ratios in previous literatures.[1,40,50] The $(EC/POC)_{FF}$ values were calculated as $(EC/POC)_{FF} = EC_{FF}/(HOC+CCOC)$. Individual HOC and CCOC values were obtained from the AMS-PMF method (see Section 2.4). For the samples without AMS-PMF data, a seasonal mean of $(EC/POC)_{FF}$ associated with an uncertainty of 30% was used, which amounted to 0.69 (0.48−0.89) and 1.25 (0.87−1.62) for wintertime and springtime samples, respectively. For samples collected during the autumn, $(EC/POC)_{FF}$ was assumed to be equal to that in spring. In summer, due to decreased contribution from coal combustion to fossil-fuel emissions as previously reported in Beijing,[51] a higher $(EC/POC)_{FF}$ of 1.9 (1.3−2.5) was used. This was slightly smaller than EC/OC emission ratios (2.1) from vehicle emission used in our previous study, which were taken from the tunnel experiments in Europe and China.[1,52,53] The uncertainties and sensitivity test of source apportionment results were carried out by the LHS methodology by generating 10 000 sets of inputs used in calculations (see Table 1).[40] Simulations with negative solutions were not included in final results and the 50th percentiles (or median) of the solution were considered as the best estimate, and the uncertainties were the 10th and 90th percentiles of the solutions.

3. RESULTS AND DISCUSSION

3.1. OC and EC Mass Concentrations. As shown in Figure 1, the annual average mass concentrations of OC and EC were 10.1 $\mu g\ m^{-3}$ (ranging from 1.9 to 33.8 $\mu g\ m^{-3}$) and 3.8 $\mu g\ m^{-3}$ (1.3−9.4 $\mu g\ m^{-3}$), respectively. OC mass concentrations were less than those for $PM_{2.5}$ samples in Beijing during 2000 (i.e., 21 $\mu g\ m^{-3}$) and 2013/2014 (i.e., 14.0 ± 11.7 $\mu g/m^3$),[33,54] whereas EC values were comparable to those reported previously (i.e., 3 $\mu g\ m^{-3}$).[33,54] The relatively lower OC mass concentrations in PM_1 than $PM_{2.5}$ is likely due to substantial contribution to $PM_{2.5}$ from larger particles such as dust and primary biogenic emissions.[55] The annual concentrations of OC and EC in PM_1 have been only reported in a few studies, and the concentrations in Beijing were significantly higher than those in Elche, Spain (i.e., OC: 3.7 ± 1.3 $\mu g\ m^{-3}$; EC: 1.5 ± 0.6 $\mu g\ m^{-3}$),[56] Brno, the Czech Republic (i.e., OC: 5.8 $\mu g\ m^{-3}$; EC: 1.6 $\mu g\ m^{-3}$)[57] and Taipei (i.e., OC:1.7 $\mu g\ m^{-3}$;

DOI: 10.1021/acs.est.7b01517
Environ. Sci. Technol. 2017, 51, 7842−7852

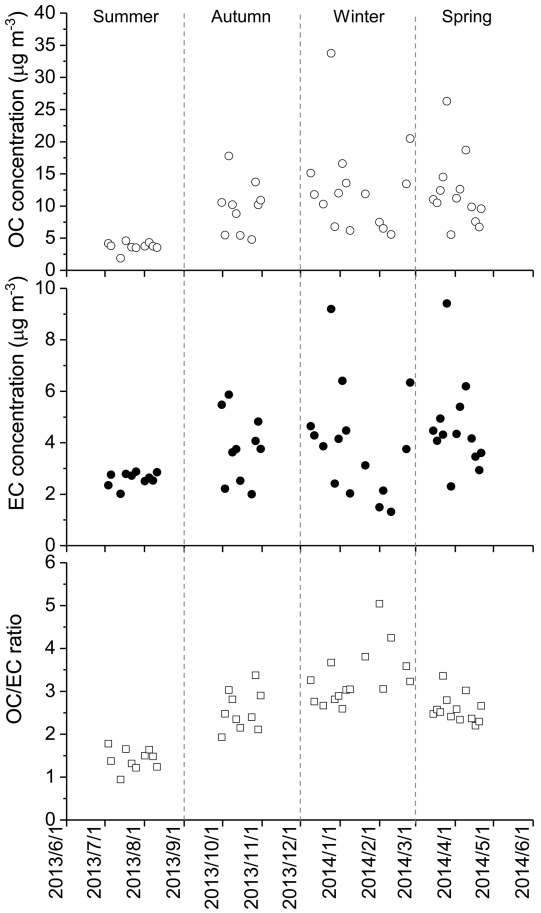

Figure 1. Temporal variations of OC and EC mass concentrations as well as OC/EC ratio of PM_1 samples in Beijing.

EC: 0.8 $\mu g\ m^{-3}$)[58] but lower than those in Xi'an (i.e., OC: 21.0 $\mu g\ m^{-3}$; EC: 5.1 $\mu g\ m^{-3}$), China.[59] The seasonal variations of OC and EC were characterized by the lowest mass concentrations in summer with a small standard derivation and the relatively higher values in other three seasons with much larger variations. As illustrated in Figure 1, both relatively high and low values in OC and EC concentrations could be occasionally observed in autumn, winter and spring although their average values were in the following order: winter = spring > autumn. It is very interesting to note that both OC and EC concentrations were very low during a long holiday season (30th January to 11th February 2014) for the Chinese Spring Festival, which was due to a large decrease in anthropogenic source emissions, for example, traffic and cooking emissions. Such a "holiday effect" has been also reported in Beijing for 2013.[60] Similar lower organic aerosols and/or EC concentrations in summer than in the other seasons were also observed previously in Beijing, which was associated with relatively high wet scavenging effects and convection due to abundant precipitation and high temperature, respectively.[34,51] The overall higher concentrations of carbonaceous aerosols in other seasons were mainly due to combined and complex effects such as increasing emissions from local and regional-transported coal and biomass/biofuel combustion and associated secondary formation as well as unfavorable metrological conditions for pollution dispersions. The relative fossil and nonfossil contributions to OC and EC will be discussed in the following sections.

3.2. Fossil and Nonfossil Sources of OC and EC.

Carbonaceous aerosol was divided into the following four categories: OC from fossil and nonfossil sources, that is, OC_{FF} and OC_{NF}, and EC from fossil and nonfossil (or biomass-burning) sources, that is, EC_{FF} and EC_{NF} (i.e., $EC_{NF} = EC_{BB}$) (see Section 2.5). Annual-average biomass -burning contribution to EC was 18 ± 7% with a range of 4−33%, suggesting a dominant contribution of fossil-fuel combustion to EC in Beijing rather than nonfossil sources. Fossil fraction in EC reported here was larger than those estimated by bottom-up inventories (i.e., 61 ± 7%) in China.[61] Such a high annual-average fossil fraction in EC is consistent with the results reported in Beijing (i.e., 79% ± 6%), China,[51] Jeju Island, Korea (i.e., 76 ± 11%),[13] and Ningbo, China (i.e., 77 ± 15%),[27] but was remarkably higher than those found in South Asia such as Hanimaadhoo, Maldives (i.e., 47 ± 9%) and Sinhagad, India (49 ± 8%)[17] as well as a background site in South China (62 ± 11%)[18] where local/regional biomass burning contribution was found to be more important than fossil fuel combustion. The biomass-burning fraction in EC was the lowest in summer (7%) and increased to around 20% during the rest of the year due to increased residential and/or open biomass-burning emissions, which was in line with a previous study for larger particles (e.g., $PM_{4.3}$) in Beijing during 2010/2011. As shown Figure 2b, fossil-derived EC was a substantial contribution of TC in summer with a mean contribution of 39 ± 3%, significantly higher than those in autumn (23 ± 5%), winter (19 ± 2%), and spring (19 ± 2%).

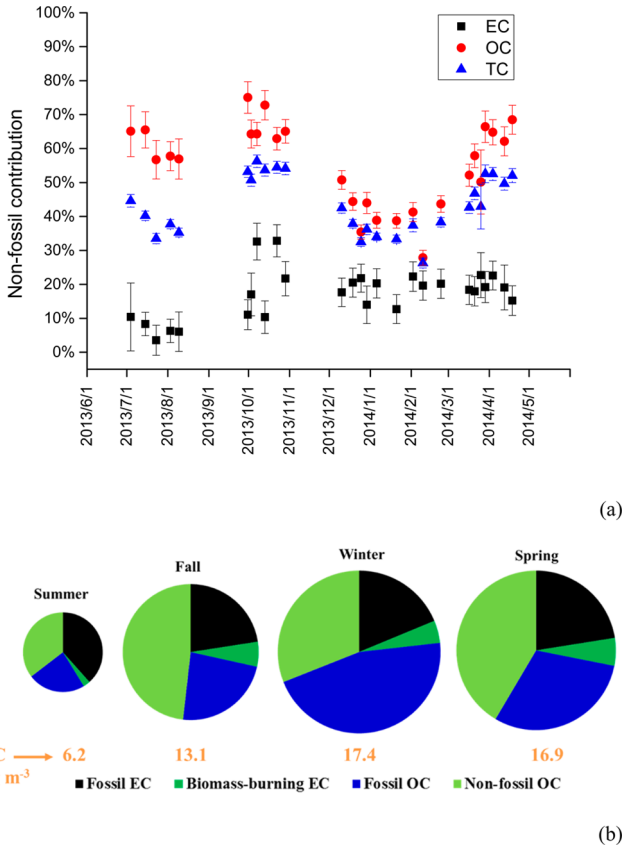

Figure 2. (a) Temporal variations of nonfossil contribution to OC, EC, and TC and (b) average source apportionment results of TC in each season of PM_1 samples in Beijing. The numbers below the pie chart represent the average TC concentrations for each season.

DOI: 10.1021/acs.est.7b01517
Environ. Sci. Technol. 2017, 51, 7842−7852

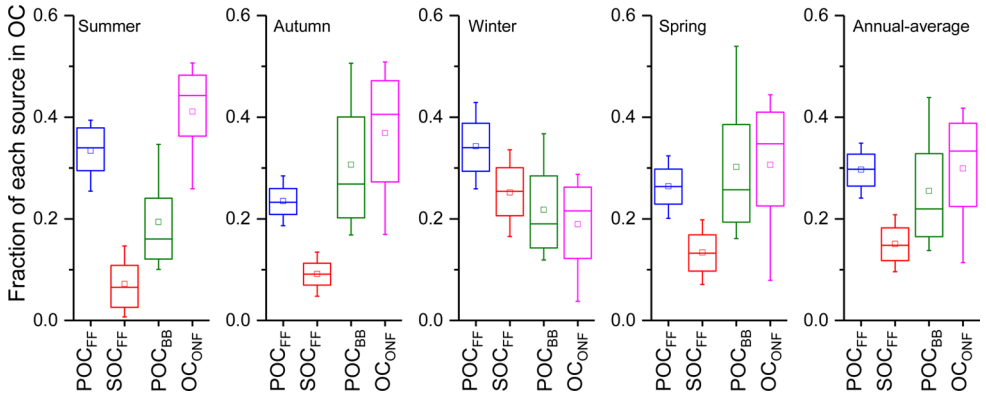

Figure 3. Fractions of each source (i.e., POC_{FF}, SOC_{FF}, POC_{BB}, OC_{ONF}) in OC of PM_1 samples in Beijing derived from the Latin-Hypercube Sampling (LHS) simulations for summer, autumn, winter, spring, and the annual-average (from left to right). The box denotes the 25th (lower line), 50th (middle line) and 75th (top line) percentiles; the empty squares within the box denote the mean values; the end of the vertical bars represents the 10th (below the box) and 90th (above the box) percentiles. POC: primary organic carbon, SOC: secondary organic carbon. FF: fossil fuel, NF: nonfossil, ONF: other nonfossil sources (details see the main text).

Nonfossil contribution to OC ranged from 28% to 75% with a mean of 52% ± 12%, which is exclusively larger than the corresponding contribution to EC (Figure 2a). This is due to relatively high contribution to OC from primary and secondary formation from nonfossil emissions such as biogenic, cooking and biomass-burning sources compared to EC. OC was dominated by nonfossil sources throughout the year except winter when a higher fossil-derived contribution for both absolute mass concentration (i.e., 8.0 ± 5.2 $\mu g\ m^{-3}$) and relative fraction (i.e., 59 ± 6%) was observed. The highest fossil-derived OC in winter was associated with enhanced coal combustions for heating during the cold periods in North China.[51,55] Interestingly, fossil fraction in EC was not higher in winter than in autumn and spring, suggesting that source pattern was not changed significantly during these three seasons.

However, the secondary formation from fossil-derived precursors may become more important and this would actually increase the fossil fraction in OC (see the next section). Indeed, the importance of SOC formation from fossil-fuel source has been previously identified in winter of Beijing and a downwind site of North China.[13,21,40] In contrast to fossil-derived OC, mass concentrations and relative contributions of nonfossil OC were higher during autumn and spring, which was very likely due to enhanced biomass-burning. The lowest nonfossil OC was observed in summer, although secondary production from biogenic emissions should be higher in this season with relatively high temperature and strong solar radiation,[13] and the overall low mass concentration was likely due to strong atmospheric convection and dispersion as explained above. The seasonal trend of the TC sources was very similar to that of OC but with a relatively lower nonfossil contribution, suggesting that total carbonaceous aerosols are largely controlled by OC emissions and formation processes.

3.3. Primary and Secondary Organic Carbon. OC contributions from POC_{BB}, OC_{ONF}, POC_{FF}, SOC_{FF} sources are displayed in Figure 3. In order to present data variability, the best estimates (the median values) as well as 10th, 25th, 75th, and 90th percentiles from the LHS simulations are also shown. On a yearly basis, the most important contributor of OC was OC_{ONF}, that is, all other nonfossil sources (i.e., 33% ± 11% for OC_{ONF}) excluding primary biomass-burning OC (POC_{BB}), mainly comprising primary and secondary biogenic OC as well as cooking OC. The highest OC_{ONF} contribution in summer was due to the increasing contributions from primary biogenic emissions and associated SOC formation with favorable atmospheric conditions (i.e., high temperature and solar radiation) as well as reduced emission for heating. OC_{ONF} contribution became lowest in winter because biogenic OC in submicron aerosols should be negligible or very small in the cold periods in North China. The mean OC_{ONF} contribution (22 ± 9%) in winter may be used as a upper limit of cooking OC, which was comparable to results resolved from AMS-PMF (~20% for COC/OC in winter, see Figure 4) in our study and also cooking contribution to organic aerosols (19 ± 4%) previously reported in Beijing.[14] The remaining OC was shared by fossil-derived POC (29 ± 4%), primary biomass-burning OC (22 ± 11%) and fossil-derived SOC (15 ± 4%). For fossil-fuel derived OC, primary emissions dominated over secondary formation in almost all cases.

A clear seasonal variation of biomass-burning source was observed with the highest contribution in autumn (27 ± 13%) and spring (26 ± 14%), followed by winter (19 ± 10%) and summer (16 ± 9%). The enhanced biomass-burning activities in autumn in Beijing and other areas in Northeast China have also been reported by measurements of biomass-burning markers such as levoglucosan and K^+ as well as stable carbon isotopic composition, which can be attributed to agricultural waste and/or fallen leaves burning.[62,63] POC_{FF} contributions were significantly higher in summer and winter. A large fraction of POC_{FF} could be from vehicle emissions elucidated by a lower mean OC_{FF}/EC_{FF} ratio in summer (i.e., mean: 0.6; range: 0.5−0.7) compared to other seasons (i.e., mean: 1.70; range: 0.5−3.8). In winter, the enhancement was observed for both the POC_{FF} (33 ± 4%) and SOC_{FF} (26 ± 10%) contributions, associated with increasing emissions from coal combustion for heating. However, the SOC contribution in PM_1 samples was obviously lower than those reported for a severe haze episode across East China in winter 2013,[40] implying relatively larger SOC contribution to $PM_{2.5}$ than PM_1.

To further investigate the relative contributions of biomass burning, cooking emissions and secondary formation to nonfossil OC, ^{14}C-based source apportionment results were integrated with AMS-PMF results. Average mass concentrations of OC determined by filter-based OC/EC analyzer and online AMS methods (OC-AMS) are shown in Figure 4. Due to

DOI: 10.1021/acs.est.7b01517
Environ. Sci. Technol. 2017, 51, 7842−7852

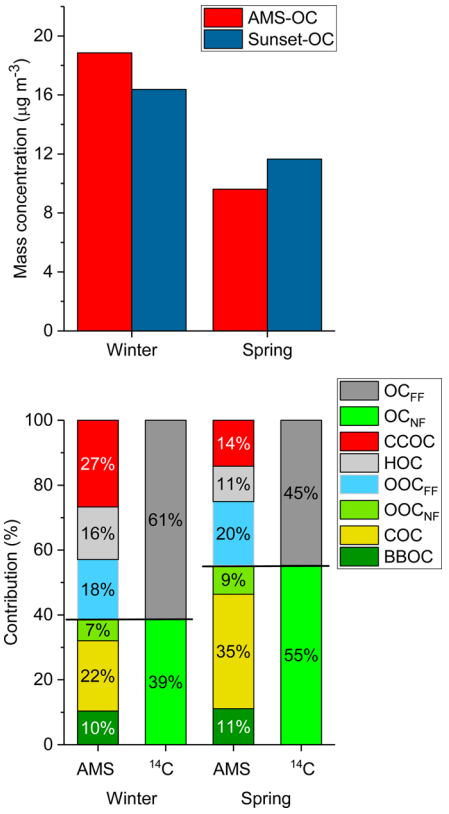

Figure 4. Average mass concentration measured by filter-based Sunset OC/EC analyzer method (OC-Sunset) and AMS method (OC-AMS) during winter (n = 4) and spring (n = 2) (top) and relative contributions to OC from different sources with a combination of ^{14}C-LHS and AMS-PMF methods (bottom). OC_{FF}: fossil-fuel derived OC; OC_{NF}: nonfossil OC; CCOC: primary coal combustion OC; HOC: hydrocarbon-like OC; OOC_{FF}: fossil-fuel oxygenated OC; OOC_{NF}: nonfossil oxygenated OC; COC: primary cooking OC; BBOC: primary biomass burning OC.

analytical uncertainties in either method, a mean OC-AMS/OC-Sunset ratio was 1.1 ± 0.2, and such a difference was also reported in other studies.[37,64] In the following, only relative contributions from each source to OC were compared to remove possible influences from differences in absolute concentrations (Figure 4). In spring and winter of Beijing, nonfossil OC was mostly derived from cooking and biomass-burning emissions. OOC, a proxy for secondary OC, comprised only a minor nonfossil fraction (15%). The results suggest that SOC was dominated by fossil fuel emissions in Beijing at least in these two seasons.

It should be noted that BBOC resolved from the AMS-PMF approach was smaller than POC_{BB} obtained from the ^{14}C-LHS method. The difference between the AMS-PMF and ^{14}C-LHS results can be explained by the uncertainties in both methods. Biomass-burning contribution may be underestimated by the AMS-PMF if aged BBOC was not included in the PMF model when biomass-burning OA was subject to substantial aging during regional transport. It may also be possible that POC_{BB} was overestimated by the ^{14}C method if a too low $(EC/POC)_{BB}$ was used in the LHS calculation, which was also reported during the DAURE campaign in Northeast Spain.[64] With a combination approach with ^{14}C and AMS-PMF methods, coal combustion was estimated to account for 62% and 56% of fossil-derived POC in winter and spring, respectively, implying an overall importance of coal combustion to OC aerosol in Beijing. The biogenic/biomass-burning derived SOC (i.e., estimated as OOC_{NF}) contributions accounted for 7% and 9% of OC in Beijing during winter and spring, respectively, demonstrating that OC was dominated by anthropogenic emissions including biomass burning, cooking emissions as well as primary and secondary OC from fossil-fuel emissions.

3.4. Fossil and Nonfossil Sources of WSOC and WIOC.

WSOC can be directly emitted as primary particles mainly from biomass burning or produced as secondary organic aerosol (SOA).[65−67] Ambient studies provide evidence that SOA produced through the oxidation of volatile organic compounds (VOCs) followed by gas-to-particle conversion contains more polar compounds and thus may be a more important source of WSOC[66−69] compared to primary organic aerosols. WSOC is therefore thought to be a good proxy of secondary organic carbon (SOC) in the absence of biomass burning.[67] The average WSOC/OC ratio in our study was 0.53 ± 0.19 (ranging from 0.21 to 0.84). And WSOC/OC mass concentration ratio and nonfossil fraction of OC (i.e., f_{NF}(OC)) show a very similar temporal variation (Figure 5)

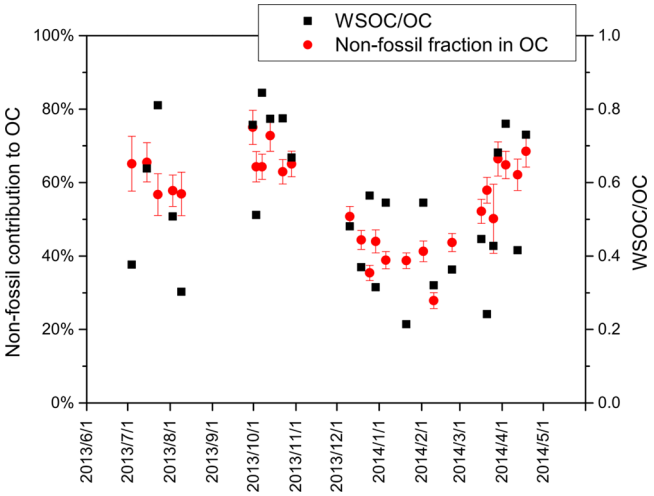

Figure 5. Temporal variations of nonfossil contribution to OC and WSOC/OC ratio of PM_1 samples in Beijing.

with a good correlation (r = 0.60, p < 0.05), indicating that nonfossil source was an important contributor of WSOC. To confirm this hypothesis, ^{14}C measurement was also performed on subfractions of OC including WSOC and water-insoluble OC (WIOC) of two samples for each season. Based on these measurements, the WSOC concentrations from nonfossil sources ($WSOC_{NF}$) ranged from 0.6 to 7.6 μg/m^3, whereas the corresponding range for WSOC from fossil-fuel emissions ($WSOC_{FF}$) was 0.5 to 11.6 μg/m^3. Nonfossil sources were major if not dominate contributors of WSOC for nearly all studied samples with a mean contribution of 58% ± 9% (Figure 6). The only exception (i.e., f_{NF}(WSOC) = 0.39) was the aerosol sample collected from 2013/12/2 to 2013/12/26 when the highest OC concentration during the whole sampling periods was observed. The highest fossil source contribution was also found for the WIOC fraction (i.e., f_{NF}(WIOC) = 0.31) for the same sample. These results showed that during this haze episode, fossil emission was the most important source of OC. $WSOC_{NF}$ can be further apportioned to WSOC from biomass

DOI: 10.1021/acs.est.7b01517
Environ. Sci. Technol. 2017, 51, 7842−7852

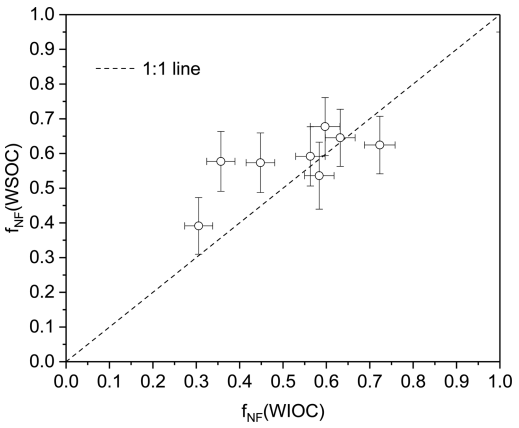

Figure 6. Relationship between f_{NF}(WSOC) and f_{NF}(WIOC).

burning (i.e., $WSOC_{BB}$) and nonfossil SOC (i.e., $WSOC_{NF,SOC}$):

$$WSOC_{NF} = WSOC_{NF,SOC} + WSOC_{BB}$$

$$WSOC_{BB} = POC_{BB} * (WSOC/OC)_{BB}$$

where POC_{BB} was previously estimated (see Section 3.3). SOC-to-OC emission ratios of biomass burning (i.e., $(WSOC\text{-to-}OC)_{BB}$) is assigned as 0.8 ± 0.2 (ranging from 0.6 to 1.0) in this study according to observations of different biomass types around the world.[65,70] Therefore, primary biomass burning and nonfossil derived SOC accounted for 62% ± 17% and 38% ± 17% of $WSOC_{NF}$, respectively. This suggest that biomass burning was generally a major contributor of nonfossil WSOC in Beijing. Furthermore, $WSOC_{FF}$ was significantly correlated (r = 0.94, p < 0.01) with SOC_{FF} (see Section 3.3), suggesting that an importance contribution of fossil-derived SOC to $WSOC_{FF}$. On the yearly basis, nonfossil contributions to WSOC were larger than those to WIOC (Figure 6), although most of the data is not statistically significant from the 1:1 line and some opposite cases were also found occasionally. Similar observations were published for other locations in Asia,[71] Europe[26] and the USA,[72] which is due to relatively high water solubility of major sources of WSOC such as biomass-burning OC and SOC that are composed of a large fraction of polar and highly oxygenated compounds.[70,73,74]

4. IMPLICATIONS

Despite dominant fossil-fuel contribution to EC particles due to large emissions from traffic and coal combustion, our study demonstrates that nonfossil emissions are generally a dominant contributor of OC including WIOC and WSOC fractions in a heavily polluted megacity in China. Such an important nonfossil contribution to OC agrees with source information identified in OC aerosols obtained in the Northern Hemisphere at urban, rural, semiurban, and background sites in Asia, Europe, and the U.S. (Figure 7). The ^{14}C-based source apportionment database shows a mean nonfossil fraction of 68 ± 13% across all sites (Figure 7). ^{14}C results of EC/TC/WSOC were not compiled for the comparisons since these carbonaceous fractions cannot fully represent OC aerosols. As discussed in the previous section, WSOC/OC ratios and nonfossil contribution of OC in Beijing have very similar temporal variations, indicating that biomass-burning emissions and biogenic-derived SOC formation were very important contributors of nonfossil OC. Indeed, WSOC/OC ratios may be also increased due to organic aerosol aging during regional and/or long-range transport, so it can be anticipated that the regional-transported nonfossil OC from rural sites to urban areas would also increase nonfossil OC fraction in urban regions. As shown in Figure 7, fossil contribution is apparently higher in the U.S. (i.e., with fossil contribution of 44 ± 11%) and East Asia (i.e., 39 ± 13%) than those observed in Europe (i.e., 25 ± 9%). This may be because most ^{14}C-based studies in the U.S. and East Asia have been conducted within, near and downwind of urban areas. Furthermore, wood burning emissions have recently become a more important contributor

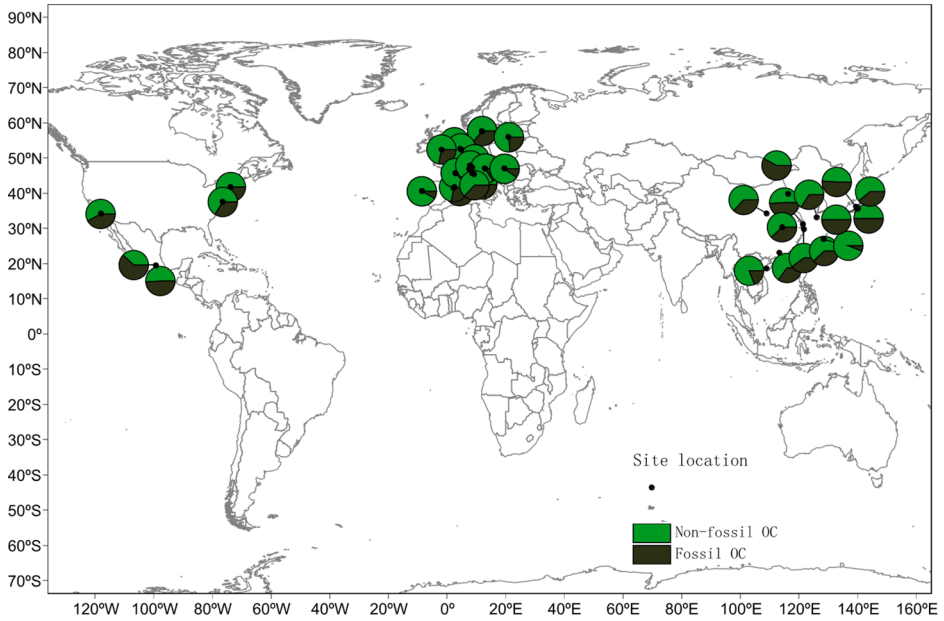

Figure 7. Fossil and nonfossil sources of OC aerosols at different locations around world. The results are obtained from this study and previous ^{14}C-source apportionment studies.[1,13,18,26−28,40,46,71,78−88] The map is created by MeteoInfo Java Edition 1.3 (http://www.meteothinker.com/).

DOI: 10.1021/acs.est.7b01517
Environ. Sci. Technol. 2017, 51, 7842−7852

of European aerosols. This would be especially the case in winter, decreasing fossil contribution.

This study shows that a combined approach of AMS-PMF and ^{14}C methods provide more comprehensive picture of the source and formation information on carbonaceous aerosols than either method alone. Therefore, such approaches are recommended to be used as a routine basis in a long-term monitoring network (e.g., at supersites) for a better source apportionment. Our study also provides a direct evidence that nonfossil source plays a major role in organic aerosol concentrations not only in rural/remote areas but also in many polluted urban sites, which seems to be contrasting to the fact that fossil fuel emissions (e.g., coal combustion and vehicle exhaust) often dominate EC aerosols (i.e., an excellent marker for primary carbonaceous aerosols) in urban areas. This unexpectedly high nonfossil contribution to OC in urban areas may be explained by urban nonfossil carbon emissions (e.g., cooking emissions and associated SOA), regional transported or locally season-dependent biomass burning emissions,[75,76] as well as biogenic/biomass-burning SOA linked with complex and combined atmospheric mechanisms such as enhancement by anthropogenic emissions.[77]

AUTHOR INFORMATION

Corresponding Authors

*(Y.Z.) Phone: +86 25 5873 1022; fax: +86 25 5873 1193; e-mail: dryanlinzhang@outlook.com or zhangyanlin@nuist.edu.cn.

*(P.F.) E-mail: fupingqing@mail.iap.ac.cn.

ORCID

Yanlin Zhang: 0000-0002-8722-8635

Yele Sun: 0000-0003-2354-0221

Notes

The authors declare no competing financial interest.

ACKNOWLEDGMENTS

This work was supported by the National Natural Science Foundation of China (Grant Nos. 91644103, 41603104, 41475117, 41571130024, 41575120), the Strategic Priority Research Program (B) of the Chinese Academy of Sciences (Grant No. XDB05030306), and the Startup Foundation for Introducing Talent of NUIST (No. 2015r023 and 2015r019) as well as Thousand Youth Talents Plan of China.

REFERENCES

(1) Gelencsér, A.; May, B.; Simpson, D.; Sánchez-Ochoa, A.; Kasper-Giebl, A.; Puxbaum, H.; Caseiro, A.; Pio, C.; Legrand, M. Source apportionment of PM2.5 organic aerosol over Europe: Primary/secondary, natural/anthropogenic, and fossil/biogenic origin. *J. Geophys. Res.* **2007**, *112* (D23), D23S04.

(2) Jimenez, J. L.; Canagaratna, M. R.; Donahue, N. M.; Prevot, A. S. H.; Zhang, Q.; Kroll, J. H.; DeCarlo, P. F.; Allan, J. D.; Coe, H.; Ng, N. L.; Aiken, A. C.; Docherty, K. S.; Ulbrich, I. M.; Grieshop, A. P.; Robinson, A. L.; Duplissy, J.; Smith, J. D.; Wilson, K. R.; Lanz, V. A.; Hueglin, C.; Sun, Y. L.; Tian, J.; Laaksonen, A.; Raatikainen, T.; Rautiainen, J.; Vaattovaara, P.; Ehn, M.; Kulmala, M.; Tomlinson, J. M.; Collins, D. R.; Cubison, M. J.; Dunlea, E. J.; Huffman, J. A.; Onasch, T. B.; Alfarra, M. R.; Williams, P. I.; Bower, K.; Kondo, Y.; Schneider, J.; Drewnick, F.; Borrmann, S.; Weimer, S.; Demerjian, K.; Salcedo, D.; Cottrell, L.; Griffin, R.; Takami, A.; Miyoshi, T.; Hatakeyama, S.; Shimono, A.; Sun, J. Y.; Zhang, Y. M.; Dzepina, K.; Kimmel, J. R.; Sueper, D.; Jayne, J. T.; Herndon, S. C.; Trimborn, A. M.; Williams, L. R.; Wood, E. C.; Middlebrook, A. M.; Kolb, C. E.; Baltensperger, U.; Worsnop, D. R. Evolution of organic aerosols in the atmosphere. *Science* **2009**, *326* (5959), 1525−1529.

(3) Mauderly, J. L.; Chow, J. C. Health effects of organic aerosols. *Inhalation Toxicol.* **2008**, *20* (3), 257−288.

(4) Highwood, E. J.; Kinnersley, R. P. When smoke gets in our eyes: The multiple impacts of atmospheric black carbon on climate, air quality and health. *Environ. Int.* **2006**, *32* (4), 560−566.

(5) IPCC. *Climate Change 2013: The Physical Science Basis. Contribution of Working Group I to the fifth Assessment Report of the Intergovernmental Panel on Climate Change*; Cambridge University Press: Cambridge, United Kingdom, 2013; p 1533.

(6) Pöschl, U. Atmospheric aerosols: composition, transformation, climate and health effects. *Angew. Chem., Int. Ed.* **2005**, *44* (46), 7520−40.

(7) Lighty, J. S.; Veranth, J. M.; Sarofim, A. F. Combustion aerosols: Factors governing their size and composition and implications to human health. *J. Air Waste Manage. Assoc.* **2000**, *50* (9), 1565−1618.

(8) Hallquist, M.; Wenger, J. C.; Baltensperger, U.; Rudich, Y.; Simpson, D.; Claeys, M.; Dommen, J.; Donahue, N. M.; George, C.; Goldstein, A. H.; Hamilton, J. F.; Herrmann, H.; Hoffmann, T.; Iinuma, Y.; Jang, M.; Jenkin, M. E.; Jimenez, J. L.; Kiendler-Scharr, A.; Maenhaut, W.; McFiggans, G.; Mentel, T. F.; Monod, A.; Prevot, A. S. H.; Seinfeld, J. H.; Surratt, J. D.; Szmigielski, R.; Wildt, J. The formation, properties and impact of secondary organic aerosol: current and emerging issues. *Atmos. Chem. Phys.* **2009**, *9* (14), 5155−5236.

(9) Fuzzi, S.; Andreae, M. O.; Huebert, B. J.; Kulmala, M.; Bond, T. C.; Boy, M.; Doherty, S. J.; Guenther, A.; Kanakidou, M.; Kawamura, K.; Kerminen, V. M.; Lohmann, U.; Russell, L. M.; Poschl, U. Critical assessment of the current state of scientific knowledge, terminology, and research needs concerning the role of organic aerosols in the atmosphere, climate, and global change. *Atmos. Chem. Phys.* **2006**, *6*, 2017−2038.

(10) Zhang, Y. L.; Kawamura, K.; Cao, F.; Lee, M. Stable carbon isotopic compositions of low-molecular-weight dicarboxylic acids, oxocarboxylic acids, α-dicarbonyls, and fatty acids: Implications for atmospheric processing of organic aerosols. *J. Geophys. Res.* **2016**, *121* (7), 3707−3717.

(11) Bond, T. C.; Doherty, S. J.; Fahey, D. W.; Forster, P. M.; Berntsen, T.; DeAngelo, B. J.; Flanner, M. G.; Ghan, S.; Karcher, B.; Koch, D.; Kinne, S.; Kondo, Y.; Quinn, P. K.; Sarofim, M. C.; Schultz, M. G.; Schulz, M.; Venkataraman, C.; Zhang, H.; Zhang, S.; Bellouin, N.; Guttikunda, S. K.; Hopke, P. K.; Jacobson, M. Z.; Kaiser, J. W.; Klimont, Z.; Lohmann, U.; Schwarz, J. P.; Shindell, D.; Storelvmo, T.; Warren, S. G.; Zender, C. S. Bounding the role of black carbon in the climate system: A scientific assessment. *J. Geophys. Res.* **2013**, *118* (11), 5380−5552.

(12) Carlton, A. G.; Wiedinmyer, C.; Kroll, J. H. A review of Secondary Organic Aerosol (SOA) formation from isoprene. *Atmos. Chem. Phys.* **2009**, *9* (14), 4987−5005.

(13) Zhang, Y. L.; Kawamura, K.; Agrios, K.; Lee, M.; Salazar, G.; Szidat, S. Fossil and Nonfossil Sources of Organic and Elemental Carbon Aerosols in the Outflow from Northeast China. *Environ. Sci. Technol.* **2016**, *50* (12), 6284−92.

(14) Hu, W.; Hu, M.; Hu, W.; Jimenez, J. L.; Yuan, B.; Chen, W.; Wang, M.; Wu, Y.; Chen, C.; Wang, Z.; Peng, J.; Zeng, L.; Shao, M. Chemical composition, sources, and aging process of submicron aerosols in Beijing: Contrast between summer and winter. *J. Geophys. Res.* **2016**, *121* (4), 1955−1977.

(15) Bond, T. C.; Streets, D. G.; Yarber, K. F.; Nelson, S. M.; Woo, J. H.; Klimont, Z. A technology-based global inventory of black and organic carbon emissions from combustion. *J. Geophys. Res.* **2004**, *109* (D14), D14203.

(16) Streets, D. G.; Bond, T. C.; Lee, T.; Jang, C. On the future of carbonaceous aerosol emissions. *J. Geophys. Res.* **2004**, *109* (D24), D24212.

(17) Sheesley, R. J.; Kirillova, E.; Andersson, A.; Krusa, M.; Praveen, P. S.; Budhavant, K.; Safai, P. D.; Rao, P. S. P.; Gustafsson, O. Year-round radiocarbon-based source apportionment of carbonaceous

DOI: 10.1021/acs.est.7b01517
Environ. Sci. Technol. 2017, 51, 7842−7852

aerosols at two background sites in South Asia. *J. Geophys. Res.* **2012**, *117*, Artn D10202.
(18) Zhang, Y.-L.; Li, J.; Zhang, G.; Zotter, P.; Huang, R.-J.; Tang, J.-H.; Wacker, L.; Prévôt, A. S. H.; Szidat, S. Radiocarbon-based source apportionment of carbonaceous aerosols at a regional background site on hainan Island, South China. *Environ. Sci. Technol.* **2014**, *48* (5), 2651−2659.
(19) Zheng, S.; Pozzer, A.; Cao, C. X.; Lelieveld, J. Long-term (2001−2012) concentrations of fine particulate matter (< sub > 2.5</ sub>) and the impact on human health in Beijing, China. *Atmos. Chem. Phys.* **2015**, *15* (10), 5715−5725.
(20) Guo, S.; Hu, M.; Zamora, M. L.; Peng, J.; Shang, D.; Zheng, J.; Du, Z.; Wu, Z.; Shao, M.; Zeng, L.; Molina, M. J.; Zhang, R. Elucidating severe urban haze formation in China. *Proc. Natl. Acad. Sci. U. S. A.* **2014**, *111* (49), 17373−8.
(21) Huang, R. J.; Zhang, Y.; Bozzetti, C.; Ho, K. F.; Cao, J. J.; Han, Y.; Daellenbach, K. R.; Slowik, J. G.; Platt, S. M.; Canonaco, F.; Zotter, P.; Wolf, R.; Pieber, S. M.; Bruns, E. A.; Crippa, M.; Ciarelli, G.; Piazzalunga, A.; Schwikowski, M.; Abbaszade, G.; Schnelle-Kreis, J.; Zimmermann, R.; An, Z.; Szidat, S.; Baltensperger, U.; El Haddad, I.; Prevot, A. S. High secondary aerosol contribution to particulate pollution during haze events in China. *Nature* **2014**, *514* (7521), 218−22.
(22) Sun, Y. L.; Du, W.; Fu, P. Q.; Wang, Q. Q.; Li, J.; Ge, X. L.; Zhang, Q.; Zhu, C. M.; Ren, L. J.; Xu, W. Q.; Zhao, J.; Han, T. T.; Worsnop, D. R.; Wang, Z. F. Primary and secondary aerosols in Beijing in winter: sources, variations and processes. *Atmos. Chem. Phys.* **2016**, *16* (13), 8309−8329.
(23) Szidat, S. Sources of Asian haze. *Science* **2009**, *323* (5913), 470−471.
(24) Heal, M. The application of carbon-14 analyses to the source apportionment of atmospheric carbonaceous particulate matter: a review. *Anal. Bioanal. Chem.* **2014**, *406* (1), 81−98.
(25) Szidat, S.; Jenk, T. M.; Synal, H.-A.; Kalberer, M.; Wacker, L.; Hajdas, I.; Kasper-Giebl, A.; Baltensperger, U. Contributions of fossil fuel, biomass-burning, and biogenic emissions to carbonaceous aerosols in Zurich as traced by ^{14}C. *J. Geophys. Res.* **2006**, *111* (D7), D07206.
(26) Zhang, Y. L.; Zotter, P.; Perron, N.; Prévôt, A. S. H.; Wacker, L.; Szidat, S. Fossil and non-fossil sources of different carbonaceous fractions in fine and coarse particles by radiocarbon measurement. *Radiocarbon* **2013**, *55* (2−3), 1510−1520.
(27) Liu, D.; Li, J.; Zhang, Y.; Xu, Y.; Liu, X.; Ding, P.; Shen, C.; Chen, Y.; Tian, C.; Zhang, G. The use of levoglucosan and radiocarbon for source apportionment of $PM_{2.5}$ carbonaceous aerosols at a background site in East China. *Environ. Sci. Technol.* **2013**, *47* (18), 10454−61.
(28) Bernardoni, V.; Calzolai, G.; Chiari, M.; Fedi, M.; Lucarelli, F.; Nava, S.; Piazzalunga, A.; Riccobono, F.; Taccetti, F.; Valli, G.; Vecchi, R. Radiocarbon analysis on organic and elemental carbon in aerosol samples and source apportionment at an urban site in Northern Italy. *J. Aerosol Sci.* **2013**, *56*, 88−99.
(29) Zhang, J. K.; Sun, Y.; Liu, Z. R.; Ji, D. S.; Hu, B.; Liu, Q.; Wang, Y. S. Characterization of submicron aerosols during a month of serious pollution in Beijing, 2013. *Atmos. Chem. Phys.* **2014**, *14* (6), 2887−2903.
(30) Zhao, P. S.; Dong, F.; He, D.; Zhao, X. J.; Zhang, X. L.; Zhang, W. Z.; Yao, Q.; Liu, H. Y. Characteristics of concentrations and chemical compositions for PM2.5 in the region of Beijing, Tianjin, and Hebei, China. *Atmos. Chem. Phys.* **2013**, *13* (9), 4631−4644.
(31) Yang, F.; Tan, J.; Zhao, Q.; Du, Z.; He, K.; Ma, Y.; Duan, F.; Chen, G.; Zhao, Q. Characteristics of $PM_{2.5}$ speciation in representative megacities and across China. *Atmos. Chem. Phys.* **2011**, *11* (11), 5207−5219.
(32) Wang, Q.; Shao, M.; Zhang, Y.; Wei, Y.; Hu, M.; Guo, S. Source apportionment of fine organic aerosols in Beijing. *Atmos. Chem. Phys.* **2009**, *9* (21), 8573−8585.
(33) Zheng, M.; Salmon, L. G.; Schauer, J. J.; Zeng, L. M.; Kiang, C. S.; Zhang, Y. H.; Cass, G. R. Seasonal trends in PM2.5 source contributions in Beijing, China. *Atmos. Environ.* **2005**, *39* (22), 3967−3976.
(34) Sun, Y. L.; Wang, Z. F.; Du, W.; Zhang, Q.; Wang, Q. Q.; Fu, P. Q.; Pan, X. L.; Li, J.; Jayne, J.; Worsnop, D. R. Long-term real-time measurements of aerosol particle composition in Beijing, China: seasonal variations, meteorological effects, and source analysis. *Atmos. Chem. Phys.* **2015**, *15* (17), 10149−10165.
(35) Sun, Y. L.; Jiang, Q.; Wang, Z. F.; Fu, P. Q.; Li, J.; Yang, T.; Yin, Y. Investigation of the sources and evolution processes of severe haze pollution in Beijing in January 2013. *J. Geophys. Res.* **2014**, *119* (7), 4380−4398.
(36) Zhang, Q.; Jimenez, J. L.; Canagaratna, M. R.; Allan, J. D.; Coe, H.; Ulbrich, I.; Alfarra, M. R.; Takami, A.; Middlebrook, A. M.; Sun, Y. L.; Dzepina, K.; Dunlea, E.; Docherty, K.; DeCarlo, P. F.; Salcedo, D.; Onasch, T.; Jayne, J. T.; Miyoshi, T.; Shimono, A.; Hatakeyama, S.; Takegawa, N.; Kondo, Y.; Schneider, J.; Drewnick, F.; Borrmann, S.; Weimer, S.; Demerjian, K.; Williams, P.; Bower, K.; Bahreini, R.; Cottrell, L.; Griffin, R. J.; Rautiainen, J.; Sun, J. Y.; Zhang, Y. M.; Worsnop, D. R. Ubiquity and dominance of oxygenated species in organic aerosols in anthropogenically-influenced Northern Hemisphere midlatitudes. *Geophys. Res. Lett.* **2007**, *34* (13), L13801.
(37) Zotter, P.; El-Haddad, I.; Zhang, Y.; Hayes, P. L.; Zhang, X.; Lin, Y.-H.; Wacker, L.; Schnelle-Kreis, J.; Abbaszade, G.; Zimmermann, R.; Surratt, J. D.; Weber, R.; Jimenez, J. L.; Szidat, S.; Baltensperger, U.; Prévôt, A. S. H. Diurnal cycle of fossil and nonfossil carbon using radiocarbon analyses during CalNex. *J. Geophys. Res.* **2014**, *119* (11), 6818−6835.
(38) Birch, M. E.; Cary, R. A. Elemental carbon-based method for monitoring occupational exposures to particulate diesel exhaust. *Aerosol Sci. Technol.* **1996**, *25* (3), 221−241.
(39) Zhang, Y. L.; Perron, N.; Ciobanu, V. G.; Zotter, P.; Minguillón, M. C.; Wacker, L.; Prévôt, A. S. H.; Baltensperger, U.; Szidat, S. On the isolation of OC and EC and the optimal strategy of radiocarbon-based source apportionment of carbonaceous aerosols. *Atmos. Chem. Phys.* **2012**, *12*, 10841−10856.
(40) Zhang, Y. L.; Huang, R. J.; El Haddad, I.; Ho, K. F.; Cao, J. J.; Han, Y.; Zotter, P.; Bozzetti, C.; Daellenbach, K. R.; Canonaco, F.; Slowik, J. G.; Salazar, G.; Schwikowski, M.; Schnelle-Kreis, J.; Abbaszade, G.; Zimmermann, R.; Baltensperger, U.; Prévôt, A. S. H.; Szidat, S. Fossil vs. non-fossil sources of fine carbonaceous aerosols in four Chinese cities during the extreme winter haze episode of 2013. *Atmos. Chem. Phys.* **2015**, *15* (3), 1299−1312.
(41) Salazar, G.; Zhang, Y. L.; Agrios, K.; Szidat, S. Development of a method for fast and automatic radiocarbon measurement of aerosol samples by online coupling of an elemental analyzer with a MICADAS AMS. *Nucl. Instrum. Methods Phys. Res., Sect. B* **2015**, *361*, 163−167.
(42) Szidat, S.; Salazar, G. A.; Vogel, E.; Battaglia, M.; Wacker, L.; Synal, H. A.; Turler, A. C-14 Analysis and Sample Preparation at the New Bern Laboratory for the Analysis of Radiocarbon with Ams (Lara). *Radiocarbon* **2014**, *56* (2), 561−566.
(43) Agrios, K.; Salazar, G.; Zhang, Y.-L.; Uglietti, C.; Battaglia, M.; Luginbühl, M.; Ciobanu, V. G.; Vonwiller, M.; Szidat, S. Online coupling of pure O2 thermo-optical methods − 14C AMS for source apportionment of carbonaceous aerosols. *Nucl. Instrum. Methods Phys. Res., Sect. B* **2015**, *361*, 288−293.
(44) Stuiver, M.; Polach, H. A. Discussion: Reporting of 14C data. *Radiocarbon* **1977**, *19* (3), 355−363.
(45) Zotter, P.; Ciobanu, V. G.; Zhang, Y. L.; El-Haddad, I.; Macchia, M.; Daellenbach, K. R.; Salazar, G. A.; Huang, R. J.; Wacker, L.; Hueglin, C.; Piazzalunga, A.; Fermo, P.; Schwikowski, M.; Baltensperger, U.; Szidat, S.; Prévôt, A. S. H. Radiocarbon analysis of elemental and organic carbon in Switzerland during winter-smog episodes from 2008 to 2012 − Part 1: Source apportionment and spatial variability. *Atmos. Chem. Phys.* **2014**, *14* (24), 13551−13570.
(46) Minguillón, M. C.; Perron, N.; Querol, X.; Szidat, S.; Fahrni, S. M.; Alastuey, A.; Jimenez, J. L.; Mohr, C.; Ortega, A. M.; Day, D. A.; Lanz, V. A.; Wacker, L.; Reche, C.; Cusack, M.; Amato, F.; Kiss, G.; Hoffer, A.; Decesari, S.; Moretti, F.; Hillamo, R.; Teinila, K.; Seco, R.; Penuelas, J.; Metzger, A.; Schallhart, S.; Muller, M.; Hansel, A.;

DOI: 10.1021/acs.est.7b01517
Environ. Sci. Technol. 2017, 51, 7842−7852

Burkhart, J. F.; Baltensperger, U.; Prevot, A. S. H. Fossil versus contemporary sources of fine elemental and organic carbonaceous particulate matter during the DAURE campaign in Northeast Spain. *Atmos. Chem. Phys.* **2011**, *11* (23), 12067−12084.
(47) Mohn, J.; Szidat, S.; Fellner, J.; Rechberger, H.; Quartier, R.; Buchmann, B.; Emmenegger, L. Determination of biogenic and fossil CO_2 emitted by waste incineration based on $^{14}CO_2$ and mass balances. *Bioresour. Technol.* **2008**, *99* (14), 6471−6479.
(48) Canagaratna, M. R.; Jimenez, J. L.; Kroll, J. H.; Chen, Q.; Kessler, S. H.; Massoli, P.; Hildebrandt Ruiz, L.; Fortner, E.; Williams, L. R.; Wilson, K. R.; Surratt, J. D.; Donahue, N. M.; Jayne, J. T.; Worsnop, D. R. Elemental ratio measurements of organic compounds using aerosol mass spectrometry: characterization, improved calibration, and implications. *Atmos. Chem. Phys.* **2015**, *15* (1), 253−272.
(49) Zhang, Q.; Jimenez, J. L.; Canagaratna, M. R.; Ulbrich, I. M.; Ng, N. L.; Worsnop, D. R.; Sun, Y. L. Understanding atmospheric organic aerosols via factor analysis of aerosol mass spectrometry: a review. *Anal. Bioanal. Chem.* **2011**, *401* (10), 3045−3067.
(50) Genberg, J.; Hyder, M.; Stenström, K.; Bergström, R.; Simpson, D.; Fors, E.; Jönsson, J. Å.; Swietlicki, E. Source apportionment of carbonaceous aerosol in southern Sweden. *Atmos. Chem. Phys.* **2011**, *11* (22), 11387−11400.
(51) Zhang, Y.-L.; Schnelle-Kreis, J. r.; Abbaszade, G. l.; Zimmermann, R.; Zotter, P.; Shen, R.-r.; Schäfer, K.; Shao, L.; Prévôt, A. S. H.; Szidat, S. n. Source apportionment of elemental carbon in Beijing, China: Insights from radiocarbon and organic marker measurements. *Environ. Sci. Technol.* **2015**, *49* (14), 8408−8415.
(52) Huang, X. F.; Yu, J. Z.; He, L. Y.; Hu, M. Size distribution characteristics of elemental carbon emitted from Chinese vehicles: Results of a tunnel study and atmospheric implications. *Environ. Sci. Technol.* **2006**, *40* (17), 5355−5360.
(53) He, L. Y.; Hu, M.; Zhang, Y. H.; Huang, X. F.; Yao, T. T. Fine particle emissions from on-road vehicles in the Zhujiang Tunnel, China. *Environ. Sci. Technol.* **2008**, *42* (12), 4461−4466.
(54) Ji, D.; Zhang, J.; He, J.; Wang, X.; Pang, B.; Liu, Z.; Wang, L.; Wang, Y. Characteristics of atmospheric organic and elemental carbon aerosols in urban Beijing, China. *Atmos. Environ.* **2016**, *125* (Part A), 293−306.
(55) Elser, M.; Huang, R. J.; Wolf, R.; Slowik, J. G.; Wang, Q.; Canonaco, F.; Li, G.; Bozzetti, C.; Daellenbach, K. R.; Huang, Y.; Zhang, R.; Li, Z.; Cao, J.; Baltensperger, U.; El-Haddad, I.; Prévôt, A. S. H. New insights into PM2.5 chemical composition and sources in two major cities in China during extreme haze events using aerosol mass spectrometry. *Atmos. Chem. Phys.* **2016**, *16* (5), 3207−3225.
(56) Yubero, E.; Galindo, N.; Nicolás, J. F.; Crespo, J.; Calzolai, G.; Lucarelli, F. Temporal variations of PM1 major components in an urban street canyon. *Environ. Sci. Pollut. Res.* **2015**, *22* (17), 13328−13335.
(57) Křůmal, K.; Mikuška, P.; Večeřa, Z. Polycyclic aromatic hydrocarbons and hopanes in PM1 aerosols in urban areas. *Atmos. Environ.* **2013**, *67*, 27−37.
(58) Cheung, H. C.; Chou, C. C. K.; Chen, M. J.; Huang, W. R.; Huang, S. H.; Tsai, C. Y.; Lee, C. S. L. Seasonal variations of ultra-fine and submicron aerosols in Taipei, Taiwan: implications for particle formation processes in a subtropical urban area. *Atmos. Chem. Phys.* **2016**, *16* (3), 1317−1330.
(59) Shen, Z.; Cao, J.; Arimoto, R.; Han, Y.; Zhu, C.; Tian, J.; Liu, S. Chemical Characteristics of Fine Particles (PM1) from Xi'an, China. *Aerosol Sci. Technol.* **2010**, *44* (6), 461−472.
(60) Jiang, Q.; Sun, Y. L.; Wang, Z.; Yin, Y. Aerosol composition and sources during the Chinese Spring Festival: fireworks, secondary aerosol, and holiday effects. *Atmos. Chem. Phys.* **2015**, *15* (11), 6023−6034.
(61) Chen, B.; Andersson, A.; Lee, M.; Kirillova, E. N.; Xiao, Q.; Krusa, M.; Shi, M.; Hu, K.; Lu, Z.; Streets, D. G.; Du, K.; Gustafsson, O. Source forensics of black carbon aerosols from China. *Environ. Sci. Technol.* **2013**, *47* (16), 9102−8.
(62) Zhang, T.; Claeys, M.; Cachier, H.; Dong, S. P.; Wang, W.; Maenhaut, W.; Liu, X. D. Identification and estimation of the biomass burning contribution to Beijing aerosol using levoglucosan as a molecular marker. *Atmos. Environ.* **2008**, *42* (29), 7013−7021.
(63) Cao, F.; Zhang, S. C.; Kawamura, K.; Zhang, Y. L. Inorganic markers, carbonaceous components and stable carbon isotope from biomass burning aerosols in Northeast China. *Sci. Total Environ.* **2016**, *572*, 1244−1251.
(64) Minguillon, M. C.; Perron, N.; Querol, X.; Szidat, S.; Fahrni, S. M.; Alastuey, A.; Jimenez, J. L.; Mohr, C.; Ortega, A. M.; Day, D. A.; Lanz, V. A.; Wacker, L.; Reche, C.; Cusack, M.; Amato, F.; Kiss, G.; Hoffer, A.; Decesari, S.; Moretti, F.; Hillamo, R.; Teinila, K.; Seco, R.; Penuelas, J.; Metzger, A.; Schallhart, S.; Muller, M.; Hansel, A.; Burkhart, J. F.; Baltensperger, U.; Prevot, A. S. H. Fossil versus contemporary sources of fine elemental and organic carbonaceous particulate matter during the DAURE campaign in Northeast Spain. *Atmos. Chem. Phys.* **2011**, *11* (23), 12067−12084.
(65) Sannigrahi, P.; Sullivan, A. P.; Weber, R. J.; Ingall, E. D. Characterization of water-soluble organic carbon in urban atmospheric aerosols using solid-state C-13 NMR spectroscopy. *Environ. Sci. Technol.* **2006**, *40* (3), 666−672.
(66) Kondo, Y.; Miyazaki, Y.; Takegawa, N.; Miyakawa, T.; Weber, R. J.; Jimenez, J. L.; Zhang, Q.; Worsnop, D. R. Oxygenated and water-soluble organic aerosols in Tokyo. *J. Geophys. Res.* **2007**, *112* (D1), D01203.
(67) Weber, R. J.; Sullivan, A. P.; Peltier, R. E.; Russell, A.; Yan, B.; Zheng, M.; de Gouw, J.; Warneke, C.; Brock, C.; Holloway, J. S.; Atlas, E. L.; Edgerton, E. A study of secondary organic aerosol formation in the anthropogenic-influenced southeastern United States. *J. Geophys. Res.* **2007**, *112* (D13), D13302.
(68) Miyazaki, Y.; Kondo, Y.; Takegawa, N.; Komazaki, Y.; Fukuda, M.; Kawamura, K.; Mochida, M.; Okuzawa, K.; Weber, R. J. Time-resolved measurements of water-soluble organic carbon in Tokyo. *J. Geophys. Res.* **2006**, *111* (D23), D23206.
(69) Hecobian, A.; Zhang, X.; Zheng, M.; Frank, N.; Edgerton, E. S.; Weber, R. J. Water-Soluble Organic Aerosol material and the light-absorption characteristics of aqueous extracts measured over the Southeastern United States. *Atmos. Chem. Phys.* **2010**, *10* (13), 5965−5977.
(70) Mayol-Bracero, O. L.; Guyon, P.; Graham, B.; Roberts, G.; Andreae, M. O.; Decesari, S.; Facchini, M. C.; Fuzzi, S.; Artaxo, P. Water-soluble organic compounds in biomass burning aerosols over Amazonia - 2. Apportionment of the chemical composition and importance of the polyacidic fraction. *J. Geophys. Res.* **2002**, *107* (D20), D8091.
(71) Kirillova, E. N.; Andersson, A.; Sheesley, R. J.; Kruså, M.; Praveen, P. S.; Budhavant, K.; Safai, P. D.; Rao, P. S. P.; Gustafsson, Ö. ^{13}C and ^{14}C-based study of sources and atmospheric processing of water-soluble organic carbon (WSOC) in South Asian aerosols. *J. Geophys. Res.* **2013**, *118* (2), 614−626.
(72) Wozniak, A. S.; Bauer, J. E.; Dickhut, R. M. Characteristics of water-soluble organic carbon associated with aerosol particles in the eastern United States. *Atmos. Environ.* **2012**, *46*, 181−188.
(73) Sullivan, A. P.; Frank, N.; Kenski, D. M.; Collett, J. L. Application of high-performance anion-exchange chromatography-pulsed amperometric detection for measuring carbohydrates in routine daily filter samples collected by a national network: 2. Examination of sugar alcohols/polyols, sugars, and anhydrosugars in the upper Midwest. *J. Geophys. Res.* **2011**, *116*, D08303.
(74) Noziere, B.; Kalberer, M.; Claeys, M.; Allan, J.; D'Anna, B.; Decesari, S.; Finessi, E.; Glasius, M.; Grgic, I.; Hamilton, J. F.; Hoffmann, T.; Iinuma, Y.; Jaoui, M.; Kahnt, A.; Kampf, C. J.; Kourtchev, I.; Maenhaut, W.; Marsden, N.; Saarikoski, S.; Schnelle-Kreis, J.; Surratt, J. D.; Szidat, S.; Szmigielski, R.; Wisthaler, A. The molecular identification of organic compounds in the atmosphere: state of the art and challenges. *Chem. Rev.* **2015**, *115* (10), 3919−83.
(75) Cheng, Y.; Engling, G.; He, K. B.; Duan, F. K.; Ma, Y. L.; Du, Z. Y.; Liu, J. M.; Zheng, M.; Weber, R. J. Biomass burning contribution to Beijing aerosol. *Atmos. Chem. Phys.* **2013**, *13* (15), 7765−7781.

DOI: 10.1021/acs.est.7b01517
Environ. Sci. Technol. 2017, 51, 7842−7852

(76) Yan, C.; Zheng, M.; Bosch, C.; Andersson, A.; Desyaterik, Y.; Sullivan, A. P.; Collett, J. L.; Zhao, B.; Wang, S.; He, K.; Gustafsson, O. Important fossil source contribution to brown carbon in Beijing during winter. *Sci. Rep.* **2017**, *7*, 43182.
(77) Hoyle, C. R.; Boy, M.; Donahue, N. M.; Fry, J. L.; Glasius, M.; Guenther, A.; Hallar, A. G.; Hartz, K. H.; Petters, M. D.; Petaja, T.; Rosenoern, T.; Sullivan, A. P. A review of the anthropogenic influence on biogenic secondary organic aerosol. *Atmos. Chem. Phys.* **2011**, *11* (1), 321−343.
(78) Liu, J.; Li, J.; Vonwiller, M.; Liu, D.; Cheng, H.; Shen, K.; Salazar, G.; Agrios, K.; Zhang, Y.; He, Q.; Ding, X.; Zhong, G.; Wang, X.; Szidat, S.; Zhang, G. The importance of non-fossil sources in carbonaceous aerosols in a megacity of central China during the 2013 winter haze episode: A source apportionment constrained by radiocarbon and organic tracers. *Atmos. Environ.* **2016**, *144*, 60−68.
(79) Szidat, S.; Ruff, M.; Perron, N.; Wacker, L.; Synal, H.-A.; Hallquist, M.; Shannigrahi, A. S.; Yttri, K. E.; Dye, C.; Simpson, D. Fossil and non-fossil sources of organic carbon (OC) and elemental carbon (EC) in Goeteborg, Sweden. *Atmos. Chem. Phys.* **2009**, *9*, 1521−1535.
(80) Wozniak, A. S.; Bauer, J. E.; Dickhut, R. M.; Xu, L.; McNichol, A. P. Isotopic characterization of aerosol organic carbon components over the eastern United States. *J. Geophys. Res.* **2012**, *117* (D13), D13303.
(81) Dusek, U.; ten Brink, H. M.; Meijer, H. A. J.; Kos, G.; Mrozek, D.; Röckmann, T.; Holzinger, R.; Weijers, E. P. The contribution of fossil sources to the organic aerosol in the Netherlands. *Atmos. Environ.* **2013**, *74*, 169−176.
(82) Zotter, P.; El-Haddad, I.; Zhang, Y.; Hayes, P. L.; Zhang, X.; Lin, Y. H.; Wacker, L.; Schnelle-Kreis, J.; Abbaszade, G.; Zimmermann, R. Diurnal cycle of fossil and nonfossil carbon using radiocarbon analyses during CalNex. *J. Geophys. Res.* **2014**, *119* (11), 6818−6835.
(83) Heal, M. R.; Naysmith, P.; Cook, G. T.; Xu, S.; Duran, T. R.; Harrison, R. M. Application of ^{14}C analyses to source apportionment of carbonaceous PM2.5 in the UK. *Atmos. Environ.* **2011**, *45* (14), 2341−2348.
(84) Aiken, a. C.; de Foy, B.; Wiedinmyer, C.; DeCarlo, P. F.; Ulbrich, I. M.; Wehrli, M. N.; Szidat, S.; Prevot, a. S. H.; Noda, J.; Wacker, L.; Volkamer, R.; Fortner, E.; Wang, J.; Laskin, a.; Shutthanandan, V.; Zheng, J.; Zhang, R.; Paredes-Miranda, G.; Arnott, W. P.; Molina, L. T.; Sosa, G.; Querol, X.; Jimenez, J. L. *Atmos. Chem. Phys. Discuss.* **2009**, *9*, 25915−25981.
(85) Ulevicius, V.; Byčenkienė, S.; Bozzetti, C.; Vlachou, A.; Plauškaitė, K.; Mordas, G.; Dudoitis, V.; Abbaszade, G.; Remeikis, V.; Garbaras, A.; Masalaite, A.; Blees, J.; Fröhlich, R.; Dällenbach, K. R.; Canonaco, F.; Slowik, J. G.; Dommen, J.; Zimmermann, R.; Schnelle-Kreis, J.; Salazar, G. A.; Agrios, K.; Szidat, S.; El Haddad, I.; Prévôt, A. S. H. Fossil and non-fossil source contributions to atmospheric carbonaceous aerosols during extreme spring grassland fires in Eastern Europe. *Atmos. Chem. Phys.* **2016**, *16* (9), 5513−5529.
(86) Gilardoni, S.; Vignati, E.; Cavalli, F.; Putaud, J. P.; Larsen, B. R.; Karl, M.; Stenström, K.; Genberg, J.; Henne, S.; Dentener, F. Better constraints on sources of carbonaceous aerosols using a combined ^{14}C−macro tracer analysis in a European rural background site. *Atmos. Chem. Phys.* **2011**, *11*, 5685−5700.
(87) Handa, D.; Nakajima, H.; Arakaki, T.; Kumata, H.; Shibata, Y.; Uchida, M. Radiocarbon analysis of BC and OC in PM10 aerosols at Cape Hedo, Okinawa, Japan, during long-range transport events from East Asian countries. *Nucl. Instrum. Methods Phys. Res., Sect. B* **2010**, *268* (7−8), 1125−1128.
(88) Fushimi, A.; Wagai, R.; Uchida, M.; Hasegawa, S.; Takahashi, K.; Kondo, M.; Hirabayashi, M.; Morino, Y.; Shibata, Y.; Ohara, T.; Kobayashi, S.; Tanabe, K. Radiocarbon (^{14}C) diurnal variations in fine particles at sites downwind from Tokyo, Japan in summer. *Environ. Sci. Technol.* **2011**, *45* (16), 6784−92.

DOI: 10.1021/acs.est.7b01517
Environ. Sci. Technol. 2017, 51, 7842−7852